npj | biological physics and mechanics

Review

https://doi.org/10.1038/s44341-025-00015-5

Premetastatic niche mechanics and organotropism in breast cancer

Sarah Libring & Cynthia A. Reinhart-King ✉

Numerous physical and mechanical changes occur in the premetastatic niche. Here, we review the mechanics of the premetastatic niche and how the altered extracellular matrix and cancer cell mechanics may play a role in organotropism in breast cancer. Future research into premetastatic niche development and organotropic cell behavior should address physical alterations and biomechanical effects to the same rigor that biochemical alterations are studied.

As the primary tumor develops, distant organs also experience cell population and extracellular composition changes in preparation for tumor cell colonization. This local supportive microenvironment is termed the premetastatic niche (PMN). The PMN broadly consists of tumor-derived secreted factors (e.g. cytokines, chemokines, extracellular vesicles), recruited bone marrow-derived cells (BMDCs) and the conversion of resident and recruited cells into cancer-associated cells (e.g. cancer-associated fibroblasts (CAFs), tumor-associated macrophages), and aberrant stroma[1]. While the concept of a PMN (i.e. fertile soil for disseminated cancer cells to seed into) is over 100 years old[2], current knowledge is lacking in understanding physical changes to the PMN, which may be unique from the mechanical changes that occur in the primary tumor microenvironment or in secondary sites after secondary tumors are established. Here, we will review current literature on the physical and mechanical alterations to the PMN that influence metastatic outgrowth in breast cancer. Given that breast cancer displays a non-random pattern of preferential metastatic locations[1], we will also discuss mechanical aspects of this preferential metastasis, termed organotropism.

Extracellular Matrix Alterations in the Premetastatic Niche

Some cancers predominantly spread to one organ, such as the propensity of pancreatic cancer to metastasize to the liver[3]. Other cancer types, particularly breast cancer and lung cancer, are able to colonize multiple organ sites. Breast cancer most commonly metastasizes to the lungs, liver, bone, and brain[3]. Tumor cell arrest appears to be dictated, in part, by the physical parameters of the circulatory system within these organs[4,5]. In the brain, circulating tumor cells (CTCs) usually arrest in areas of low flow at vascular branch points within the capillary bed[4,6]. In the lungs, CTCs become lodged in the distal arterial pulmonary circulation as vessels naturally narrow. Given that the basal regions of the lungs are more highly vascularized, hematogenous metastases prominently appear in the basal region[7]. Similarly, due to its size, high vascularization, and role in filtration, CTCs may become lodged in the small capillaries of the liver. However, vessel diameter and flow rate are not the only physical parameters at play, as cancer cells have been found to attach to one side of blood vessels that are larger than the tumor cell diameter, particularly in sinusoids[5,8]. In both the bone marrow and the liver, this sinusoidal vasculature is fenestrated and there is a lack of organized continuous basement membrane. Therefore, these locations are thought to be more permissive to CTC extravasation, thus lessening the requirement for size-based entrapment[3,9]. Additionally, PMN priming of particular organs appears to alter metastatic outgrowth patterns from those predicted purely by circulation mechanics, as the altered tissue niches enable disseminated tumor cells to successfully extravasate, evade immune detection, and begin proliferating. Extracellular matrix (ECM) alterations in PMNs typically include accumulation of matrix proteins and increased crosslinking—resulting in overall matrix stiffening, disruption to the basement membranes, and an increase in vasculature growth and leakiness. Matrix accumulation observed in the PMN includes collagens (such as type I[10–12] and type 14[13,14]), but seems mainly related to glycoproteins—including fibronectin[15–19], tenascin C[17,19–21], and periostin[7,20], among others[22].

Crosslinking Agents and Induced Fibrosis

Molecules secreted at the primary tumor that have been extensively studied in altering the primary tumor matrix may also arrive at and alter distant tissues to form PMNs. For example, during primary tumor progression, particularly when primary tumors are under hypoxia, overexpressed hypoxia-inducible factor 1 alpha (HIF-1α) leads to the release of lysyl oxidase (LOX) in a P2Y2 receptor-dependent manner[23]. Secreted LOX and LOX-like (LOXL) proteins can crosslink fibers (collagens, elastin) and the LOX family has been extensively reviewed in development and in the primary tumor microenvironment[24,25]. Erler et al. showed that mice with orthotopic injections of MDA-MB-231 triple-negative breast cancer cells with a LOX shRNA knockdown had reduced lung metastases and reduced presence of BMDCs in the lungs[16]. The premetastatic lungs of mice inoculated with wildtype MDA-MB-231 cells showed increased fibronectin deposition in the terminal bronchioles and distal alveoli, with LOX co-localized exclusively to this fibronectin, compared to the lungs of mice inoculated with LOX-deficient cells[16]. Narciso et al. also demonstrated that fibronectin deposition was correlated to regions of high hypoxia and

Department of Bioengineering, Rice University, Houston, TX, USA. ✉e-mail: Cynthia.Reinhart-King@rice.edu

necrosis in metastatic lesions[26] and Wu et al. showed that conditioned media from LOXL2 over-expressing hepatocellular carcinoma cells or media supplemented with recombinant LOXL2 (rhLOXL2) upregulated fibronectin production in lung fibroblasts[18]. Similarly, mice with orthotopic injections of MDA-MB-231 cells with HIF-1α knockdown had both reduced collagen crosslinks in the lungs and reduced lung metastasis compared to mice with wildtype tumor cells[23,27]. However, Cai et al. found downregulation of LOX in premetastatic lungs and in breast cancer-conditioned lung fibroblasts[13]. This was explained by the difference in primary tumor size, wherein the mice under Cai et al. had relatively small tumors (~ 260 mm^3) with presumably less hypoxia[13], although a smaller primary tumor size does not guarantee less hypoxia/necrosis[28]. Moreover, primary tumor size does not explain the downregulation of LOX seen in fibroblasts cultured with MDA-MB-231-conditioned media as compared to control fibroblasts[13]. We propose that this is likely due to the presence of serum in the MDA-MB-231 media, where other studies often switch to serum-free media as the base for conditioned media collection. Prolonged serum deprivation was shown to induce HIF-1α in prostate cancer cells irrespective of oxygen conditions[29]. This indicates that PMN accumulation of matrix proteins and matrix crosslinking proteins may be induced by several mechanisms beyond hypoxia at the tumor core, but future work is needed to understand the mechanisms fully.

Several studies have attempted to isolate the impact of a fibrotic PMN on metastatic potential. In one, BALB/c mice underwent bleomycin treatment or thoracic irradiation to induce pulmonary fibrosis, or Dimethylnitrosamine treatment to induce hepatic fibrosis[30]. PMN fibrosis did not affect primary tumor growth, but mice with induced PMN fibrosis had an approximately 2.5 fold larger pulmonary metastatic burden than control mice. A similar effect was seen in pulmonary metastatic burden after tail vein injection (as opposed to orthotopic injection) in fibrotic and control mice. In subsequent studies, mice were treated with an anti-LOX antibody or an IgG control for 3 weeks after chemical- or irradiation-induced fibrosis, stopping 48 h prior to orthotopic injection of 4T1 cells. No difference in primary tumor growth was seen, while anti-LOX treated mice had an approximately 50% reduction in pulmonary metastatic burden and a significant reduction in frequency of hepatic metastasis across the individual experiments[30]. Barkan et al. performed a complementary study on the isolated impact of a fibrotic PMN. Here, CD1/nu/nu athymic mice received an adenoviral vector expressing active Transforming Growth Factor Beta 1 (TGFß1) to the lungs to induce fibrosis. 21 days post-infection, D2.0 R cells were injected in the tail vein, and the lungs were analyzed 4 weeks post-injection[10]. Typically, D2.0 R cells disseminate, but remain dormant for months, with only occasional completion of macrometastases[10,31]. Following TGFß1 treatment, the mouse lungs became fibrotic, with increased deposition of matrix that included type I collagen. Total tumor burden per lung was 18-fold higher in mice with fibrotic lungs than mice that received an empty adenoviral vector. The authors observed that this increase was not due to TGFß1 signaling directly, but that the collagen-I (and fibronectin) enriched lungs induced a phenotypic switch (i.e. dormant to proliferative) in the D2.0 R cells, mediated by the cells' ß1 integrin expression[10,32]. In total, the isolated development of fibrosis in PMNs seems to increase metastatic outgrowth. However, the effect of PMN fibrosis on breast cancer cell dissemination or arrest from circulation into metastatic niches is unclear. When pulmonary fibrosis was induced physically (e.g. through irradiation), there was no effect on the number of disseminated tumor cells initially lodged within the lungs 2 h post tail-vein injection, but the fibrotic environment supported subsequent survival and proliferation of these lodged tumor cells to form micrometastases, with the presence of multicell clusters appearing in only fibrotic mice after 72 h[30]. In contrast, when spontaneous-tumor-forming mice (MMTV-PyMT background) were genetically altered to carry a mammary gland-specific deletion of LOXL2, the number of CTCs in the peripheral blood was significantly reduced compared to control mice[19]. Perhaps unsurprisingly, this demonstrates that crosslinking at the primary tumor site and premetastatic sites have different effects on the efficiency of individual steps of the metastatic cascade, although both result in a heavy reduction in metastatic incidence (incidence was 75% lower in mice without mammary gland LOXL2 than control mice[19]).

It is important to note that the induction of a fibrotic PMN does not solely affect the ECM. Following bleomycin treatment in vitro, Cox et al. observed elevated alpha-smooth muscle actin (αSMA) expression and LOX secretion from fibroblasts on collagen[30]. In fact, matrix accumulation and stiffening via crosslinking (elastic modulus measured via shear rheology) were considered downstream events of fibroblast activation[30]. Tumor-secreted LOXL2 (via 4T1 cells) was also shown to activate fibroblasts into a more CAF-like phenotype in the tumor microenvironment[33] and increase BMDC recruitment to premetastatic sites, such that intracellular effects of LOX and LOXL2 may initially promote breast cancer cell invasion and CAF formation only then to be followed by extracellular LOX acting on ECM stiffness[19]. Stiffer, more rigid matrices may then influence other cells in the PMN, creating a positive stiffening feedback loop through LOX family members. For example, a recent report showed that stiffer matrices strengthened M2 macrophage polarization and promoted expression of additional LOXL2 through HIF-1α upregulation in liver cancer models[34,35]. Increased Young's modulus of the matrix by activated fibroblasts was also sufficient to increase 4T1 proliferation rates without the continued presence of the fibroblasts themselves in the constructs[30]. However, clinically, simtuzumab, a LOXL2-specific blocking monoclonal antibody, has not shown benefit in reducing fibrosis or altering metastatic pancreatic adenocarcinoma patient outcomes[36,37]. There may be innumerable reasons for this, stemming from formulation issues to timing of when treatment starts relative to fibrotic and metastatic progression, but it is also possible that another LOX family member is a more suitable target against premetastatic fibrosis and/or metastatic progression. In particular, LOXL4 has gained attention recently, but results have been mixed whether increased LOXL4 expression is beneficial or deleterious for metastatic progression[34,37–40].

Additionally, the LOX family are not the only matrix crosslinking agents. Fibrillar fibronectin can be stabilized via *o,o'*-dityrosine crosslinking under reducing conditions (although soluble fibronectin cannot undergo fibrillogenesis this way). Interestingly, this reaction was driven by TGFß1 and required the presence of myeloperoxidase, which is derived from inflammatory cells[41]. Tissues also stiffen through the nonenzymatic formation of advanced glycation end-products (AGEs), which accumulate through age and during certain conditions, such as diabetes[42,43]. Increased crosslinking generally reduces tissue viscoelasticity by limiting fiber-fiber/fibril-fibril sliding under tensile or compressive forces[44]. In a spontaneous tumor-forming mouse model, hyperglycemia did not alter the accumulation of collagen at the primary tumor, but did increase AGEs, resulting in an increase in breast tumor stiffness compared to nondiabetic mice. Stiffness was quantified as tissue equilibrium modulus after unconfined compression testing (poroviscoelastic model) and elastic modulus via atomic force microscopy[45]. Glycation-based stiffening has also been shown to increase tumor cell proliferation, mesenchymal phenotype, and invasion, suggesting disease advancement, but AGE accumulation in PMN development or metastatic outcomes have not been reported yet (particularly in a mechanical sense, separate from cellular AGE-RAGE (Receptor for AGEs) pathways), with pilot studies on AGE-breakers for cancer just beginning[42,45–49]. Lastly, transglutaminase 2 (TG2) has the ability to crosslink both intracellular and extracellular proteins, in addition to regulating several cellular functions biochemically[50]. In the ECM, TG2 acts as a transamidase, where it can associate with several proteins, including crosslinking collagen fibrils and stabilizing the basement membrane through laminin-nidogen complex crosslinks[51,52]. TG2 expression is often downregulated in primary tumors but upregulated in association with secondary metastases, and is associated with lower overall survival clinically[53,54]. Additionally, TG2 inhibitors were shown to sensitize various cancer cells to chemotherapeutics, in part, by disrupting fibronectin assembly in the ECM[54]. TG2 has been found in/on extracellular vesicles from multiple metastatic breast cancer cell lines, where the molecule crosslinked fibronectin on the vesicle surface, and contributed to the activation of fibroblasts (when coupled with fibronectin) in the tumor microenvironment after extracellular vesicle

uptake[55–57]. Specifically, the N-terminal domain of TG2 binds to the gelatin-binding domain of fibronectin (FN42), whereby this TG2/fibronectin complex then provides a binding site for ß1 and ß3 integrins, leading to cell adhesion and a host of downstream effects[51]. Of note, this is somewhat similar to indirect pathways noted by both tenascin C and periostin—both can co-assemble with fibronectin and modulate its adhesiveness and stiffness, which ultimately alters the integrin signaling capacity of the fibrillar network[58]. In addition, TG2 binding to fibronectin was recently found to be tuned by the mechanical tension of the fibers (with affinity for low-tension fibronectin fibers), such that the TG2/fibronectin complex could be considered a mechanoregulator, but much more work is needed to identify extracellular roles of TG2 (aka tissue transglutaminase 2 when acting extracellularly) in PMN development[51,59].

Metastatic Lesion Stiffness Over Time

It is known that the mechanical properties of secondary sites will impose changes on disseminated cancer cells upon arrival. Breast cancer relapse is often detected in tissues that have lower elastic moduli than the normal mammary gland or the primary breast tumor, such as the bone marrow and the brain[60]. Breast cancer cells in the lung microenvironment will also experience unfamiliar cyclic stretching, which appears to inhibit proliferation until matrix degradation, creating pockets of low strain, is achieved[61]. Perhaps this explains why breast cancer cells with greater metastatic potential were observed to have greater intracellular viscoelastic plasticity—i.e. an ability to quickly alter intracellular mechanics. Specifically, even within a spheroid of cells of similar origin, the 4T1 cells that displayed the largest invasion (i.e. leader cells) behaved in a more viscous manner as compared to those retained in the spheroid center. This was measured by comparing the scaling exponent α of the cytoplasm via optical tweezers. The authors also observed that the α value and the apparent Young's modulus (measured via real time deformability cytometry) of invasive cell lines (including MDA-MB-231 and 4T1 cells) were more likely to vary with substrate stiffness/density (1 and 4 mg/ml collagen gels) compared to the noninvasive cell lines (including MCF7 and 67NR cells)[62]. Relatedly, cancer cells with greater metastatic potential were observed to be less sensitive to stiffness changes when grown on fibronectin-coated polyacrylamide hydrogels, surviving and growing regardless of environmental stiffness cues[63]. However, cell behavior was not consistent, with MDA-MB-231 cells having a lower α (more elastic) and higher Young's modulus in 4 mg/ml collagen gels, and 4T1 cells having a higher α (more viscous) and lower Young's modulus in 4 mg/ml gels compared to 1 mg/ml gels[62], making global interpretation difficult.

Although global PMN development appears to revolve around tissue stiffening, no studies have yet analyzed the micromechanical properties of the ECM around metastatic lesions in breast cancer over time. Narciso et al. have, however, measured such for melanoma (and lung cancer) cells arriving in the lungs after tail vein injection[26]. Metastases were subdivided as micro- or macrometastases based on size. The ECM surrounding melanoma micrometastases appeared to be disorganized, degraded lung ECM, with the alveoli and blood vessels still occasionally intact/visible. In comparison, macrometastases were surrounded by a thick layer of ECM (referred to as a capsule) and the tumor was confined within the borders of the capsule. These "ECM-rich" areas comprised approximately 5% of the total area of each macrometastasis. Healthy (decellularized) lung tissue had a Young's modulus of approximately 0.4 kPa measured by atomic force microscopy (Fig. 1a). Of note, the healthy tissue values were taken from tumor-adjacent ECM, as opposed to separate control mice, but it had likely not gone through a broader PMN development because cancer cells were intravenously injected in these experiments. Surprisingly, the ECM of decellularized micrometastases was significantly softer than healthy ECM, with a Young's modulus of approximately 0.2 kPa. In contrast, decellularized macrometastases were significantly stiffer than healthy lung ECM, with the ECM-rich regions being more than 15-fold stiffer (approximately 6.4 kPa) (Fig. 1a). In total, the smallest micrometastases are within a healthy lung ECM range, but progressively soften (measured by Young's modulus) as they enlarge until, around 0.5 mm^3, when the metastases become encapsulated and develop an ECM-rich region surrounding the growing tumor of cells (Fig. 1b). As expected, this increase in Young's modulus was related, in part, to altered ECM composition. Micrometastases had a slight increase in fibronectin signal (approximately 118% of baseline healthy signal). Perhaps unexpectedly, while the ECM-rich regions of macrometastases were significantly overexpressed for fibronectin (approximately 250% of baseline), the total tumor levels of fibronectin showed a decrease to approximately 88% of baseline[26]. This is similar to the transient increase in total fibronectin signal that we have seen in the premetastatic lung niche of BALB/c mice after orthotopic injection of 4T1 cells (Fig. 1c, d)[15], and highlights the need for more research specifically parsing the dynamics of the metastatic lesions compared to the greater PMN.

Mechanical Mechanisms of Organotropism

Breast Cancer Subtypes and Organotropic Metastasis

Although percentages vary by study given differing demographics and follow-up times, it is now well established that the different subtypes of breast cancer have different metastatic behaviors. Table 1 displays the patient counts for single site metastatic locations from two recent manuscripts[64,65]. We calculated the percentages as the number of patients within a breast cancer subtype with a given metastatic location against the number of total patients in that subtype, in order to compare the two studies. These studies agree with others that estrogen receptor-positive (ER +) breast cancer patients have an increased likelihood of developing bone metastases, while triple-negative breast cancer patients are at an increased risk of developing visceral metastases[66–68]. It has been shown that triple-negative breast cancer patients still experience lower overall survival than other breast cancer patients when controlling for the same site of metastases (e.g. bone-only metastasis and brain-only metastasis)[64,69]. Medeiros et al. demonstrated that a unique premetastatic lung niche was established in nude mice using a triple-negative cell line (SUM159) as compared to a luminal A cell line (MCF7), including enhanced expression of periostin, fibronectin, tenascin-c, and MMP-9 (matrix metalloproteinase). When breast cancer cells were exposed in vitro to lung-conditioned media from mice bearing SUM159 tumors, migration and proliferation rates increased. This was not seen in breast cancer cells grown in lung-conditioned media from mice bearing MCF7 tumors, demonstrating that the developed triple-negative premetastatic lung niche itself has soluble factors that can enhance breast cancer cell survival and growth[20]. Further work from this lab has demonstrated that exposing breast cancer cells to lung-conditioned media from mice bearing triple-negative tumors increased the proportion of $ALDH^{hi}/CD44^{+}$ cells in the population and supported stemness/plasticity in the cancer cell population[70]. As MCF7 cells are considered low/non-metastatic (Table 2), whether the PMN created is primarily a function of breast cancer subtype or metastatic potential is difficult to decouple, and may not be possible given that different subtypes have different metastatic potentials clinically. Instead, it may be advantageous to study why luminal breast cancers, although having a lower early metastatic risk[71], have a relative increased risk of bone metastases. Wang et al. observed that breast cancer cells can form contact-dependent E-cadherin—N-cadherin heterotypic adherens junctions with alkaline phosphatase-positive (ALP +) osteogenic cells in the early metastatic bone niche, which conferred a proliferation advantage on the disseminated tumor cells. Given that E-cadherin is the major cadherin in the luminal subtype, this unique PMN interaction may contribute to the increased clinical bone metastases[72]. In a 2019 review, Gao et al. theorized that breast cancer subtypes may utilize different mechanisms from one another to achieve bone metastases. This includes the heterotypic adherens junctions for ER+ breast cancer, while ER- studies report more PMN bone priming—i.e. promoting osteoclast activity through secreted factors—although secretion of CXCL12 or homing to CXCL12-rich regions appears common across subtypes[73]. Many aspects of metastatic organotropism, such as cancer cell-released soluble chemoattractants, are beyond the scope of this review (but can be found in other recent reviews[1,74,75]), while

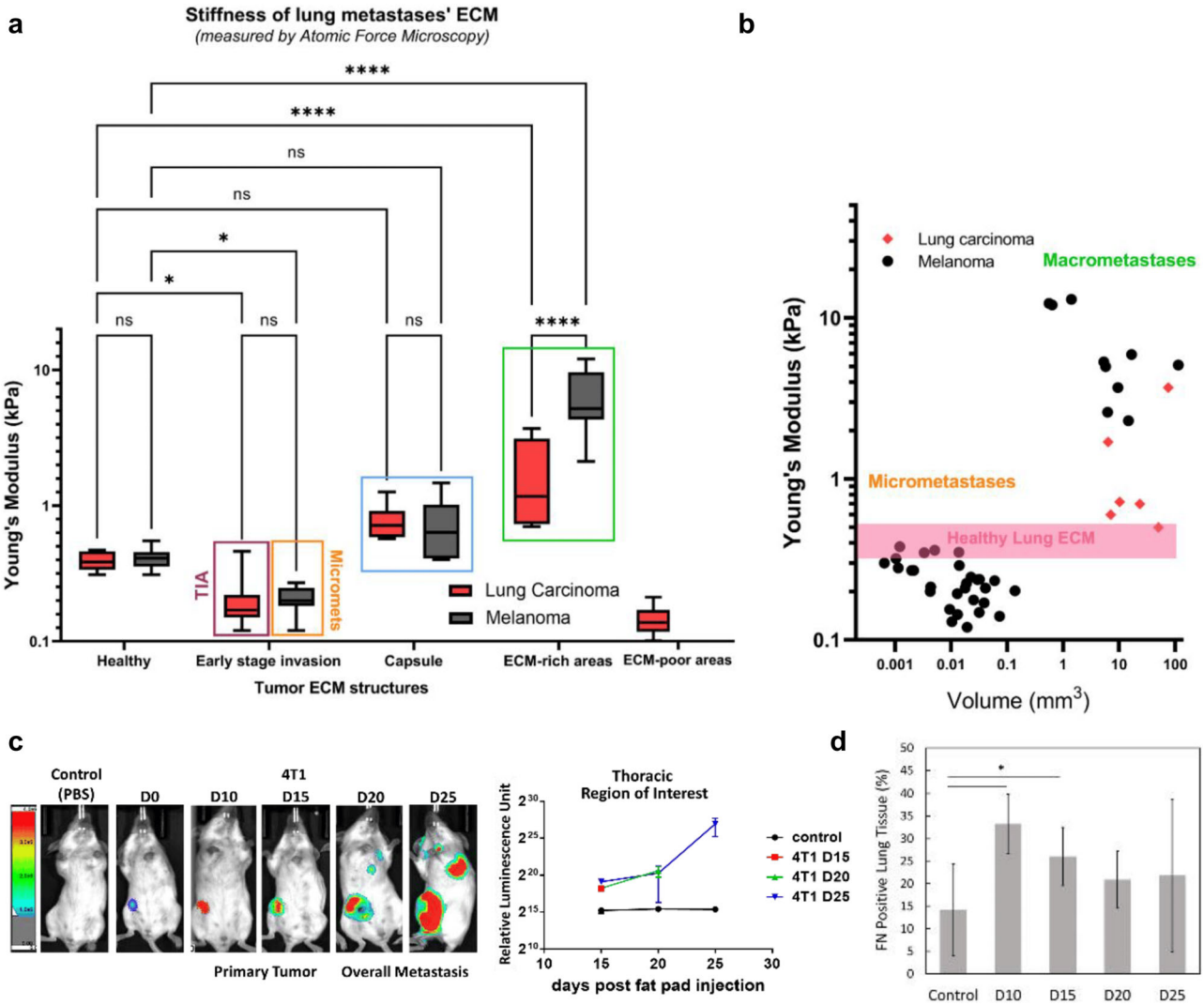

Fig. 1 | Mechanics of the premetastatic niche and metastatic lesions. a Young's modulus (kPa) of healthy and metastatic lung extracellular matrix (ECM), measured by atomic force microscopy, showed significant softening during melanoma micrometastasis stage (orange box), and significant stiffening of the ECM-rich areas for melanoma macrometastases (green box). TIA stands for tumor-infiltrating area of lung carcinoma samples. (ns: $p > 0.05$; *: $p < 0.05$; ****: $p < 0.0001$). **b** Young's modulus of metastases plotted against their size. **c** Primary tumor growth and metastatic progression of 4T1 cells following orthotopic injection, tracked using bioluminescence. Days 10 and 15 represent PMN conditions, with days 20 and 25 showing overt metastasis. **d** Fibronectin signal quantification from immunohistochemical staining of the lungs shows a transient increase correlated with the PMN. (*: $p < 0.05$). **a**, **b** adapted from Narciso et al.[26] and **c**, **d** adapted from Libring et al.[15] under CC BY 4.0.

organotropism in the context of disseminated tumor cell mechanical properties is discussed below.

Tumor Cell Mechanics and Organotropic Metastasis

The mechanical properties of a cell are mainly determined by its actin filaments, intermediate filaments, and microtubules related to the cytoskeleton[76] and by the mechanical properties of its organelles, particularly the nucleus[77]. Several studies have found that transformed mammary epithelial cells have a lower Young's modulus than their normal predecessors. Among heterogeneous tumor cell populations, more invasive tumor cells have the lowest Young's modulus, and tumor cells with a soft cytoskeleton and reduced F-actin assembly have enhanced survival under shear force and increased stemness[28,60,78–88]. Beyond these differences, however, recent studies suggest that secondary tumor cells at different locations have distinct mechanical properties from each other. Tang et al. observed that breast cancer cells with bone tropism (i.e. a propensity to metastasize to the bone) had a higher Young's modulus (measured via atomic force microscopy) with enhanced F-actin in the cell cytoskeleton compared with breast cancer cells with brain tropism or the parental MDA-MB-231 cells[78]. In contrast, another study did not find a significant difference in Young's modulus via atomic force microscopy measurements between bone-tropic, brain-tropic, and parental MDA-MB-231 lines. However, bone-tropic MDA-MB-231 cells did have a larger area of tyrosine-phosphorylated paxillin focal adhesions and phosphorylated-focal adhesion kinase (FAK)-rich focal adhesions on the collagen I substrate than the parental and brain-tropic lines, and the sublines had differences in cell morphology from one another and with respect to morphological changes across substrates of varied stiffnesses[89]. Given these conflicting results, whether cell elasticity itself is innate to organotropism is unclear, and the differences may be due to the experimental design of the studies, but is likely also because these do not appear to be the same organ-tropic sublines, indicating that differences in stiffness seen among the Memorial Sloan Kettering-based sublines[78] may be byproduct and not a driver of organotropic behavior. Continuing their work, Tang et al. modified the mechanics of the brain-tropic or bone-tropic cell sublines and characterized shifts in the brain-tropic or bone-tropic genes associated with each subline[78]. For

Table 1 | Total number (top) and percentage (bottom) of patients with single site metastasis to bone, liver, lung, or brain, segmented by breast cancer subtype

	Single Site Metastasis							
	Bone		Liver		Lung		Brain	
Luminal A HR + /HER2-	2144	178	194	69	335	85	27	6
	79.4%	52.7%	7.2%	20.4%	12.4%	25.1%	1.0%	1.8%
Luminal B HR + /HER2+	304	452	113	265	63	299	7	32
	62.4%	43.1%	23.2%	25.3%	12.9%	28.5%	1.4%	3.1%
HR-/HER2+	112	150	131	148	80	189	14	20
	33.2%	29.6%	38.9%	29.2%	23.7%	37.3%	4.2%	3.9%
Triple-Negative	243	155	106	87	257	156	35	23
	37.9%	36.8%	16.5%	20.7%	40.1%	37.1%	5.5%	5.5%

Number of patients were obtained from Guo et al.[64] (left of each metastatic location column) and Fan et al.[65] (right of each metastatic location column)
Percentage was recalculated here, to determine the percent of patients within each subtype that presented with a particular single site metastatic location, for better comparison between studies. Percentages in left or right) columns add to 100% within each subtype row, with rounding tolerance. Abbreviations: HR (Hormone Receptor). The hormones referred to are estrogen and progesterone. HER2 (Human Epidermal Growth Factor Receptor 2).

example, inhibiting Rho-associated protein kinase (ROCK) in the bone-tropic cells with Y27632 had a minimal effect on the levels of most bone-tropic genes, but resulted in an upregulation of some brain-tropic genes (*LTBP1, PIEZO2, EREG*, and *ITGB3*) (Fig. 2a). However, the effect in changed gene signature was not consistent depending on the pharmacological intervention used (Y27632, F-actin inhibitor Cytochalasin D, or myosin II inhibitor blebbistatin) and was also somewhat different than the result when mDia1, a downstream effector of RhoA, was knocked down (Fig. 2b), making it difficult to generalize a conclusion[78] on innate cell elasticity and organotropism.

Lastly, in the generation of these organ-tropic cell series, parental breast cancer cells were allowed to metastasize and the metastatic populations were isolated and serially inoculated in additional mice until stable organ-tropic sublines were established, which is a standard methodology[78,89,90]. However, because these organ-tropic sublines have already been through the entire metastatic cascade numerous times, it is unclear if they were an intrinsic, present population within the mechanical heterogeneity of the original primary tumor that best survived in a correspondingly stiff or soft PMN, or whether these cells adopted the characteristics of said environments and became more organotropic during secondary tumor development after non-specific lodging in a secondary location. Several approaches attempt to answer the question of whether an organ-homing subpopulation is present in a naïve primary tumor. Savci-Heijink et al. analyzed 157 primary breast tumors from patients with known metastatic disease to determine a 15-gene signature that predicts for bone metastases (*APOPEC3B, ATL2, BBS1, C6orf61, C6orf167, MMS22L, KCNS1, MFAP3L, NIP7, NUP155, PALM2, PH-4, PGD5, SFT2D2 and STEAP3)*[91] and a 14-gene signature that predicts for visceral metastases (*WDR6*, *CDYL*, *ATP6V0A4*, *CHAD*, *IDUA*, *MYL5*, *PREP*, *RTN4IP1*, *BTG2*, *TPRG1*, *ABHD14A*, *KIF18A*, *S100PBP*, and *BEND3)*[92] indicating that the cells of the primary tumor already have alterations that indicate organotropic behavior. In total, it seems that organotropic behavior can be identified in naïve primary tumors, such as from patient sample biopsies that have not undergone serial metastasis to create organotropic sublines. Whether the correlation of tumor cell elastic modulus, specifically, is a byproduct or in itself a driving force of organotropism remains an active area of investigation by several groups. The establishment of soft and stiff sublines sorted from a parental line in vitro and subsequent in vivo testing of metastatic potential and organotropism may be a new avenue of research to further illuminate this distinction.

It is also important to note that a cell's viscoelastic behavior is not the only mechanical aspect that may affect metastatic potential and organotropism. Since CTCs must successfully reattach to the endothelium under fluid shear stress before extravasating, Zhang et al. recently demonstrated that this process selects for tumor cells with enhanced adhesion strength[93].

Arrest of CTCs is often a two-step process. Initially, adhesion receptors on the surface of CTCs, such as CD44 and integrin $\alpha_v ß_3$, facilitate a weak adhesion to endothelial cells (e.g. E-selectin). A strong adhesion develops during the rolling of cancer cells on the endothelium via integrin $\alpha_5 ß_1$[5,93,94]. Specifically, the rolling of cancer cells along a microvessel wall induces a localized vortex in the fluid flow. Due to the vortex, the rolling cell/cluster can experience plasma flow that is twice the otherwise maximum flow, wherein this higher shear force activates adhesion molecules on the surrounding platelets and on the cancer cells. 80 pN is the critical adhesion force necessary for CTCs to initiate adhesion to the endothelium, corresponding to a fluid flow of 450 μm/s[6,95]. Kang et al. demonstrated that it may be possible to reduce hematogenous metastasis of HR-/ER-/CD44+ breast cancer cells by inhibiting their ability to adhere to E-selectin-expressing blood vessels. This was done through a single injection of an E-selectin targeted aptamer, after which metastasis was reduced in MDA-MB-231 and 4T1 orthotopic models[96]. Other adhesion molecules, such as intercellular adhesion molecule 1 (ICAM-1) and vascular cell adhesion molecule 1 (VCAM-1), have been found in disseminated breast cancer cells, wherein higher expression is correlated with disseminated tumor cell survival and increased metastasis. In some recent studies, these molecules appear more to modulate tumor-tumor cell adhesion and macrophage-tumor cell adhesion of circulating clusters, respectively, rather than driving arrest and extravasation through endothelial cell-tumor cell adhesion, but this is still under active investigation and may be cancer type and/or model specific[97–101].

Vascular endothelial cells have also been recently shown to be unique across different organs[102]. Therefore, it is possible that subsets of CTCs may adhere better to certain types of endothelial cells, driving organotropism through differential tumor cell-endothelial cell adhesion profiles and extravasation ability. Zhang et al. developed an in vitro chip to mimic the brain endothelium and observed that the MDA-MB-231 cells that preferentially adhered to the human brain endothelial cell layer expressed higher levels of genes typically seen in brain metastases[93]. Importantly, cells that were allowed to adhere to the brain endothelium without exposure to shear stress (1 dyne/cm^2 wall shear stress for 15 min) did not obtain the enhanced brain metastasis characteristics, implicating that organotropic selection requires a physical component[93]. Whether a similar correlation exists between endothelium adhesion to other model organs and the presence of organ-specific metastatic gene signatures in adherent cells is yet unknown.

Lastly, a greater emphasis is likely needed on understanding biomechanical changes induced by fluid shear stress, especially by the lymphatic system. Pereira et al. observed that lung metastases contained breast cancer cells that entered the bloodstream after sentinel lymph node colonization[103]. Naxerova et al. similarly demonstrated through colorectal

Table 2 | Comparison of breast cancer cell lines mentioned throughout this review paper

Cell Line	Subtype	Origin	Phenotype	Migratory/Invasive	Metastatic Potential
MCF7	Luminal A	Derived from a pleural effusion in a female Caucasian patient with invasive ductal carcinoma who had undergone radiotherapy and Diethylstilbestrol hormone therapy	Epithelial-like	None (-)	None (-)
MDA-MB-231	Triple-Negative	Derived from a pleural effusion in a female Caucasian patient with invasive ductal carcinoma who had undergone chemotherapy	Mesenchymal-like (heterogeneous)	Very (+++)	Some (++)
SUM159	Triple-Negative	Derived from a primary anaplastic breast carcinoma in a female Caucasian patient who had not undergone chemotherapy	Mesenchymal-like, with a high proportion of stem-like cells	Some (++)	Some (++)
4T1	Triple-Negative	Derived from a spontaneous mammary tumor (410.4 tumor) in a MMTV + BALB/c mouse foster nursed on a C3H mother	Epithelial-like (heterogeneous)	Very (+++)	Very (+++)
67NR	Triple-Negative		Mesenchymal-like	Little (+)	None (-)
MCF10Ca1a	Triple-Negative	MCF10A cells (origin: benign breast tissue from a female with fibrocystic breast disease) were transfected with T24 *HRAS*, and one carcinoma (clone MCF10AT1K.cl2) was used for trocar transplantation of 1 mm^3 tumor pieces or organoids in nude-beige mice to produce the Ca1a and Ca1h cell lines, respectively	Epithelial-like	Little (+)	Little (+)
MCF10Ca1h	Triple-Negative		Mesenchymal-like	Some (++)	None (-) or Little (+)
D2.A1	Triple-Negative	D2 hyperplastic alveolar nodules (D2HAN) were inoculated orthotopically in BALB/c mice, giving rise to mammary tumors that generated lung macrometastases or failed to metastasize for the D2.A1 and D2.0 R cell lines, respectively	Mesenchymal-like	Some (++)	Some (++)
D2.0 R	Triple-Negative		Epithelial-like, growth arrest on soft substrates	Little (+)	None (-) or Little (+)

The exact phenotype, invasion, and metastasis seen will vary depending on the experimental setup. Given that each cell line can grow sufficiently on 2D plastic, migratory/invasive behavior is characterized in 3D matrices, such as in collagen I gels. Note: this is not a comprehensive list of all cells used in the referenced papers or all available breast cancer cell lines.

cancer clonal evolution studies that distant metastases and lymph node metastases often share a common origin, as compared to the primary tumor cells[104]. In vitro, lymphatic-like wall shear stress levels (0.05 dyne/cm^2) activated YAP/TAZ signaling in prostate cancer CTCs[105–107]. Additionally, cancer cells were increasingly more motile, with a higher velocity during migration, after exposure to wall shear stress values of 0.05, 0.5, and 1 dyne/cm^2, but no boost in motility was observed after exposure to a larger wall shear stress more representative of hematogenous metastasis (5 dyne/cm^2)[106]. Kawai et al. demonstrated that lymphatic endothelial cells that were exposed to 0.5 or 1 dyne/cm^2 shear stress had increased ICAM-1 expression, which accelerated the attachment of cancer cells to the lymphatics. This indicates that heightened shear stress exposure on some lymphatic endothelial cells (due to other vessels around the primary tumor collapsing) may help drive the formation of the sentinel lymph node[108]. Together, these results suggest that the mechanics and cellular interactions that disseminated cancer cells experience during lymph involvement prior to circulation may play a critical role in enhancing final survival and colonization in secondary locations, but much more study is required to elucidate such a potential role in breast cancer.

Conclusion

In total, great strides have been made in understanding the physical and mechanical properties of PMNs and mechanical components of organotropism (Fig. 3). Broadly, the premetastatic niche matrix appears to stiffen prior to outgrowth and as metastases grow large, but may soften around micrometastases. Regarding cell mechanics, while it is known that breast cancer cells have a lower Young's modulus than non-transformed cells, and grow softer with increased aggressive behavior, it is still debated whether organotropic sublines display different mechanical properties, such as viscoelasticity and adhesion strength, and, moreover, whether differences reported by some are a byproduct or a driving force in organotropic behavior.

Much work has gone into analyzing the PMN developed by breast cancer cells with the greatest metastatic potential. It is important to note, however, that the subpopulation of tumor cells that comprises the bulk of metastatic nodules may not be the primary subpopulation that conditions the PMN. Within our work, we have observed that the mesenchymal, migratory MCF10CA1h cell line could not form overt metastases in vivo and did not make up a significant portion of the metastases formed when orthotopically co-injected with epithelial MCF10CA1a cells[109], but did appear to be the primary source of extracellular vesicles that could re-educate resident lung fibroblasts to produce a more fibrotic matrix[15]. In a mathematical model of niche construction and metastasis, two types of tumor cells appear within the primary tumor; similar to the MCF10CA1h and MCF10CA1a cells, the types were cells that contribute to niche construction at their own cost and those that reap the benefits without contributing, which were termed producers and cheaters, respectively[110]. Complementarily, research has indicated that, in breast cancer, outgrowth of single lodged cancer cells into detectable metastatic lesions is the primary rate-limiting step of metastasis, not the ability to disseminate[111–114]. Thus, future work on PMN development should focus on how the altered microenvironment facilitates or inhibits colonization of the organ after extravasation, not necessarily how the mechanics affect arrest from circulation, although work on mechanics-based organ-specific homing is likely relevant[115,116]. When analyzing the mechanics of the developing PMN itself, the tissue appears to stiffen, partly through accumulation of matrix proteins such as fibronectin, and largely due to increased crosslinking. Once metastases begin to grow, there is evidence that the ECM around micrometastases may soften as the small lesions grow, driven by ECM degradation. This potentially critical, but transient reduction in local ECM stiffness may be related to the mesenchymal-to-epithelial transition of disseminated tumor cells and overall metastatic potential. Therefore, future work on PMN development and metastatic outgrowth should likely focus on the interactions between single disseminated tumor cells and the cellular and extracellular components of the PMN that reinitiate proliferation, with an

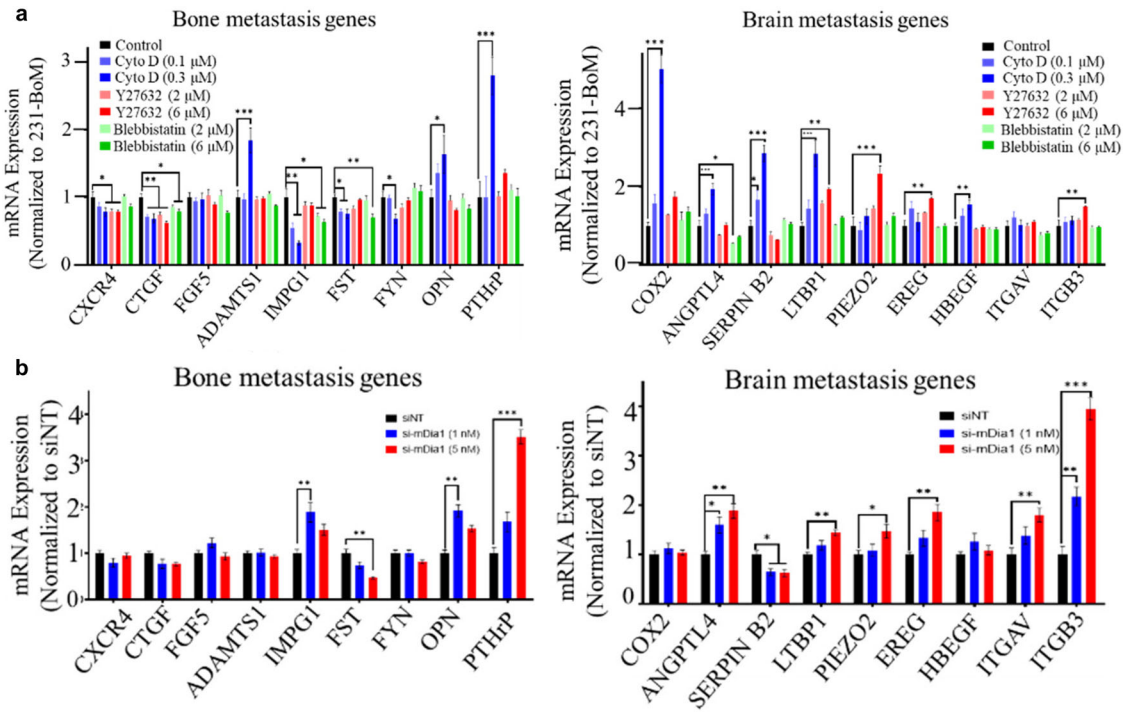

Fig. 2 | Expression of organ-tropic genes is altered when cell mechanics are altered. mRNA expression of canonical bone-metastasis genes (left) and brain-metastasis genes (right) in MDA-MB-231 bone-tropic subline after (**a**) pharmacologically disrupting cell mechanics (24 hours) or (**b**) knocking down mDia1, a downstream effector of RhoA and key driver for actin polymerization. Y27632 is a ROCK inhibitor; Cytochalasin D (Cyto D) is an F-actin inhibitor, and Blebbistatin is a myosin II inhibitor. Values measured by real time-polymerase chain reaction (RT-PCR). *: $p < 0.05$; **: $p < 0.01$; and *** p: < 0.001. Figure adapted from Tang et al.[78] under CC BY 4.0.

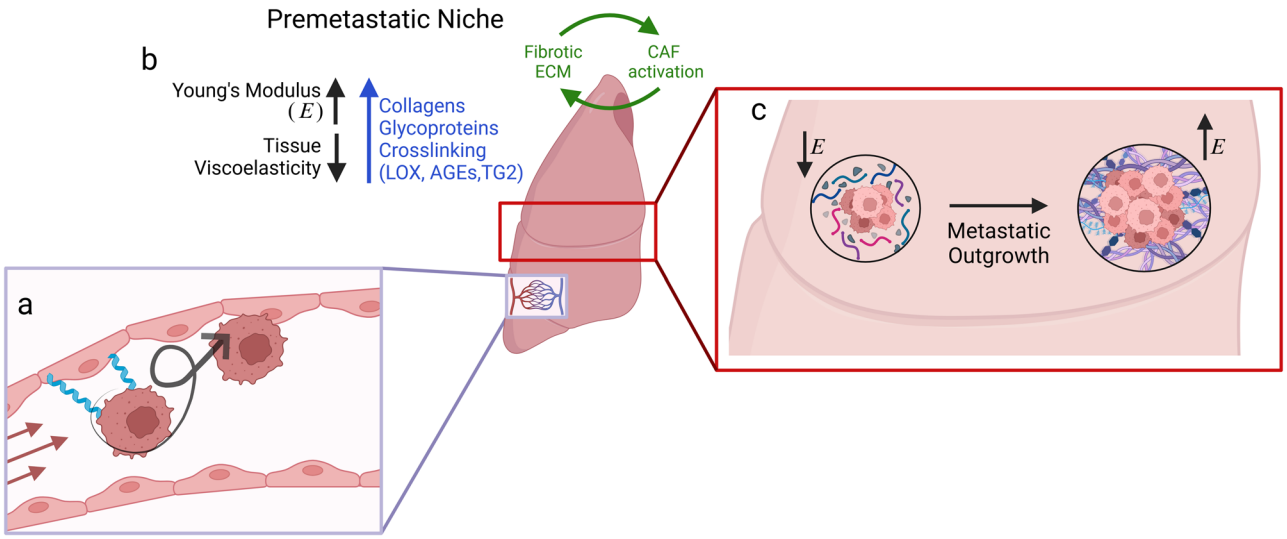

Fig. 3 | Summary of main mechanics in the premetastatic niche. a Extravasation may select for circulating tumor cells (CTCs) with enhanced adhesion strength. Adhesion is a two-step process in which CTCs first weakly adhere to endothelial cells, then begin to roll, creating a localized vortex in fluid flow that activates stronger adhesion molecules. Organotropism may be affected by unique adhesion profiles of CTCs with endothelial cells of various organs. **b** Global premetastatic niche (PMN) development appears to revolve around tissue stiffening, with an increased Young's modulus and decrease in tissue viscoelasticity due to the accumulation of matrix proteins and increased crosslinks. A fibrotic PMN activates stromal cells, creating a feedback loop, and is ultimately associated with increased metastasis. **c** However, micrometastases may have a lower Young's modulus than the surrounding tissue due to disorganized, degraded matrix. Macrometastases then develop ECM-rich capsules with high Young's moduli, mimicking the primary tumor. Intracellularly, metastatic potential is correlated with lower Young's modulus and high viscoelastic plasticity, which may enable the cells survive across these varied stages of the metastatic cascade that with changing forces and mechanics (e.g. shear in circulation, cyclic stretching in the lungs, various tissue elastic moduli). Created with BioRender.com.

emphasis on the phenotypic, metabolic, and mechanical plasticity of the breast cancer cells[117–120]. Discoveries here may enable a new area of therapeutics which aim not to reduce dissemination from the primary tumor or target actively dividing cells, but force already-disseminated cells to remain asymptomatic indefinitely.

Data Availability

No datasets were generated or analysed during the current study.

Abbreviations

ABHD14A	Abhydrolase Domain Containing 14A
AGE	Advanced Glycation End-Product
ALDH	Aldehyde Dehydrogenase
APOPEC3B	Apolipoprotein B mRNA editing enzyme, catalytic polypeptide-like 3B
αSMA	alpha-Smooth Muscle Actin
ATL2	Atlastin GTPase 2 (ATL2)
ATP6V0A4	ATPase, H+ transporting, lysosomal V0 subunit a4
BBS1	Bardet-Biedl syndrome 1
BEND3	BEN domain containing 3
BMDC	Bone Marrow Derived Cells
BTG2	BTG Anti-Proliferation Factor 2
CAF	Cancer-Associated Fibroblast
CD1	Cluster of Differentiation 1 (gene cluster that encodes a family of glycoproteins)
CDYL	Chromodomain protein, Y-like
CHAD	Chondroadherin
CTC	Circulating Tumor Cell
CXCL12	C-X-C motif Chemokine Ligand 12 (aka stromal cell-derived factor 1 (SDF-1))
C6org167	Chromosome 6 open reading frame 167
C6org61	Chromosome 16 open reading frame 61
ECM	Extracellular Matrix
ER	Estrogen Receptor
EREG	Epiregulin
FAK	Focal Adhesion Kinase
HER2	Human Epidermal Growth Factor Receptor 2
HIF-1α	Hypoxia-Inducible Factor 1 alpha
HR	Hormone Receptor
ICAM-1	Intercellular Adhesion Molecule 1
IDUA	Alpha-L-iduronidase
ITGB3	Integrin Subunit Beta 3
KIF18A	Kinesin Family Member 18A
KCNS1	Potassium voltage-gated channel, delayed-rectifier, subfamily S, member 1
LOX	Lysyl Oxidase
LOXL	Lysyl-Oxidase-like protein
LTBP1	Latent Transforming Growth Factor Beta-binding Protein 1
mDIA1	Diaphanous-related Formin (aka Protein Diaphanous Homolog 1 (DIAP1))
MFAP3L	Microfibrillar-associated protein 3-like
MMP	Matrix metalloproteinase
MMS22L	E3 ubiquitin-protein ligase substrate receptor MMS22-like protein
MYL5	Myosin, light chain 5, regulatory
NIP7	Nuclear import 7 homolog (S. cerevisiae)
NUP155	Nucleoporin 155 kDa
PALM2	Paralemmin 2
PGD5	PiggyBac transposable element derived 5
PH-4	Hypoxia-inducible factor prolyl 4-hydroxylase
PIEZO2	Piezo Type Mechanosensitive Ion Channel Component 2
PMN	Premetastatic Niche
PR	Progesterone Receptor
PREP	Prolyl Endopeptidase
P2Y2 Receptor	P2Y Purinoceptor 2 Receptor (aka P2RY2)
RAGE	Receptor for AGE
RHOA	Ras Homolog Family Member A
ROCK	Rho-associated Protein Kinase
RTN4IP1	Reticulon 4 interacting protein 1
SFT2D2	SFT2 domain containing 2
shRNA	Short hairpin RNA
STEAP3	STEAP family member 3
S100PBP	S100P (Calcium Binding Protein P) Binding Protein
TAZ	Transcriptional Co-activator with PDZ Binding Motif
TGFß1	Transforming Growth Factor Beta 1
TG2	Transglutaminase 2
TPRG1	Tumor Protein p63 Regulated 1
VCAM-1	Vascular Cell Adhesion Molecule 1
WDR6	WD Repeat Domain 6
YAP	Yes-Associated Protein

Received: 5 September 2024; Accepted: 14 February 2025;
Published online: 03 April 2025

References

1. Li, Y. et al. Pre-metastatic niche: from revealing the molecular and cellular mechanisms to the clinical applications in breast cancer metastasis. *Theranostics* **13**, 2301–2318 (2023).
2. Psaila, B. & Lyden, D. The metastatic niche: adapting the foreign soil. *Nat. Rev. Cancer* **9**, 285–293 (2009).
3. Obenauf, A. C. & Massagué, J. Surviving at a distance: organ specific metastasis. *Trends Cancer* **1**, 76–91 (2015).
4. Wrobel, J. K. & Toborek, M. Blood–brain barrier remodeling during brain metastasis formation. *Mol. Med.* **22**, 32–40 (2016).
5. Ma, R. et al. Mechanisms involved in breast cancer liver metastasis. *J. Transl. Med.* **13**, 64 (2015).
6. Follain, G. et al. Hemodynamic forces tune the arrest, adhesion, and extravasation of circulating tumor cells. *Dev. Cell* **45**, 33–52.e12 (2018).
7. Stella, G. M., Kolling, S., Benvenuti, S. & Bortolotto, C. Lung-seeking metastases. *Cancers* **11**, 1010 (2019).
8. Haier, J., Korb, T., Hotz, B., Spiegel, H.-U. & Senninger, N. An intravital model to monitor steps of metastatic tumor cell adhesion within the hepatic microcirculation. *J. Gastrointest. Surg. J. Soc. Surg. Aliment. Trac.* **7**, 507–515 (2003).
9. Inoue, S. & Osmond, D. G. Basement membrane of mouse bone marrow sinusoids shows distinctive structure and proteoglycan composition: a high resolution ultrastructural study. *Anat. Rec.* **264**, 294–304 (2001).
10. Barkan, D. et al. Metastatic growth from dormant cells induced by a Col-I enriched fibrotic environment. *Cancer Res.* **70**, 5706–5716 (2010).
11. Paidi, S. K. et al. Label-free Raman spectroscopy detects stromal adaptations in pre-metastatic lungs primed by breast cancer. *Cancer Res.* **77**, 247–256 (2017).
12. Cohen, N. et al. Breast cancer–secreted factors promote lung metastasis by signaling systemically to induce a fibrotic premetastatic niche. *Cancer Res.* **83**, 3354–3367 (2023).
13. Cai, R. et al. Primary breast tumor induced extracellular matrix remodeling in premetastatic lungs. *Sci. Rep.* **13**, 18566 (2023).
14. Goto, R., Nakamura, Y., Takami, T., Sanke, T. & Tozuka, Z. Quantitative LC-MS/MS analysis of proteins involved in metastasis of breast cancer. *PLoS ONE* **10**, e0130760 (2015).
15. Libring, S. et al. The dynamic relationship of breast cancer cells and fibroblasts in fibronectin accumulation at primary and metastatic tumor sites. *Cancers* **12**, 1270 (2020).
16. Erler, J. T. et al. Hypoxia-induced lysyl oxidase is a critical mediator of bone marrow cell recruitment to form the pre-metastatic niche. *Cancer Cell* **15**, 35–44 (2009).

17. Kaplan, R. N. et al. VEGFR1-positive haematopoietic bone marrow progenitors initiate the pre-metastatic niche. *Nature* **438**, 820–827 (2005).
18. Wu, S. et al. Matrix stiffness-upregulated LOXL2 promotes fibronectin production, MMP9 and CXCL12 expression and BMDCs recruitment to assist pre-metastatic niche formation. *J. Exp. Clin. Cancer Res.* **37**, 99 (2018).
19. Salvador, F. et al. Lysyl oxidase-like protein LOXL2 promotes lung metastasis of breast cancer. *Cancer Res.* **77**, 5846–5859 (2017).
20. Medeiros, B. et al. Triple-negative primary breast tumors induce supportive premetastatic changes in the extracellular matrix and soluble components of the lung microenvironment. *Cancers* **12**, 172 (2020).
21. Oskarsson, T. et al. Breast cancer cells produce tenascin C as a metastatic niche component to colonize the lungs. *Nat. Med.* **17**, 867–874 (2011).
22. Winkler, J., Abisoye-Ogunniyan, A., Metcalf, K. J. & Werb, Z. Concepts of extracellular matrix remodelling in tumour progression and metastasis. *Nat. Commun.* **11**, 5120 (2020).
23. Joo, Y. N. et al. P2Y2R activation by nucleotides released from the highly metastatic breast cancer cell contributes to pre-metastatic niche formation by mediating lysyl oxidase secretion, collagen crosslinking, and monocyte recruitment. *Oncotarget* **5**, 9322–9334 (2014).
24. Amendola, P. G., Reuten, R. & Erler, J. T. Interplay between LOX enzymes and integrins in the tumor microenvironment. *Cancers* **11**, 729 (2019).
25. Wei, S., Gao, L., Wu, C., Qin, F. & Yuan, J. Role of the lysyl oxidase family in organ development (Review). *Exp. Ther. Med.* **20**, 163–172 (2020).
26. Narciso, M. et al. Lung Micrometastases Display ECM Depletion and Softening While Macrometastases Are 30-Fold Stiffer and Enriched in Fibronectin. *Cancers* **15**, 2404 (2023).
27. Wong, C. C.-L. et al. Hypoxia-inducible factor 1 is a master regulator of breast cancer metastatic niche formation. *Proc. Natl. Acad. Sci. USA* **108**, 16369–16374 (2011).
28. Katara, G. K. et al. Mammary epithelium-specific inactivation of V-ATPase reduces stiffness of extracellular matrix and enhances metastasis of breast cancer. *Mol. Oncol.* **12**, 208–223 (2018).
29. Thomas, R. & Kim, M. H. HIF-1α: A key survival factor for serum-deprived prostate cancer cells. *Prostate* **68**, 1405–1415 (2008).
30. Cox, T. R. et al. LOX-mediated collagen crosslinking is responsible for fibrosis-enhanced metastasis. *Cancer Res.* **73**, 1721–1732 (2013).
31. Prunier, C. et al. Breast cancer dormancy is associated with a 4NG1 state and not senescence. *NPJ Breast Cancer* **7**, 140 (2021).
32. Barkan, D. et al. Inhibition of metastatic outgrowth from single dormant tumor cells by targeting the cytoskeleton. *Cancer Res* **68**, 6241–6250 (2008).
33. Barker, H. E., Bird, D., Lang, G. & Erler, J. T. Tumor-secreted LOXL2 activates fibroblasts through FAK signaling. *Mol. Cancer Res.* **11**, 1425–1436 (2013).
34. Lewinska, M. et al. Fibroblast-derived lysyl oxidase increases oxidative phosphorylation and stemness in cholangiocarcinoma. *Gastroenterology* **166**, 886–901.e7 (2024).
35. Xing, X. et al. Matrix stiffness-mediated effects on macrophages polarization and their LOXL2 expression. *FEBS J.* **288**, 3465–3477 (2021).
36. Benson, A. B. et al. A phase II randomized, double-blind, placebo-controlled study of simtuzumab or placebo in combination with gemcitabine for the first-line treatment of pancreatic adenocarcinoma. *Oncologist* **22**, 241–e15 (2017).
37. Ma, H.-Y. et al. LOXL4, but not LOXL2, is the critical determinant of pathological collagen cross-linking and fibrosis in the lung. *Sci. Adv.* **9**, eadf0133 (2023).
38. Barker, H. E., Cox, T. R. & Erler, J. T. The rationale for targeting the LOX family in cancer. *Nat. Rev. Cancer* **12**, 540–552 (2012).
39. Sebban, S., Davidson, B. & Reich, R. Lysyl oxidase-like 4 is alternatively spliced in an anatomic site-specific manner in tumors involving the serosal cavities. *Virchows Arch. Int. J. Pathol.* **454**, 71–79 (2009).
40. Choi, S. K., Kim, H. S., Jin, T. & Moon, W. K. LOXL4 knockdown enhances tumor growth and lung metastasis through collagen-dependent extracellular matrix changes in triple-negative breast cancer. *Oncotarget* **8**, 11977–11989 (2017).
41. Locy, M. L. et al. Oxidative crosslinking of fibronectin confers protease resistance and inhibits cellular migration. *Sci. Signal*. **13**, (2020).
42. Palanissami, G. & Paul, S. F. D. AGEs and RAGE: metabolic and molecular signatures of the glycation-inflammation axis in malignant or metastatic cancers. *Explor. Target. Anti-Tumor Ther.* **4**, 812–849 (2023).
43. Marino, G. E. & Weeraratna, A. T. A glitch in the matrix: Age-dependent changes in the extracellular matrix facilitate common sites of metastasis. *Aging Cancer* **1**, 19–29 (2020).
44. Gautieri, A. et al. Advanced glycation end-products: Mechanics of aged collagen from molecule to tissue. *Matrix Biol.* **59**, 95–108 (2017).
45. Wang, W. et al. Diabetic hyperglycemia promotes primary tumor progression through glycation-induced tumor extracellular matrix stiffening. *Sci. Adv.* **8**, eabo1673 (2022).
46. Rowe, M. M., Wang, W., Taufalele, P. V. & Reinhart-King, C. A. AGE-breaker ALT711 reverses glycation-mediated cancer cell migration. *Soft Matter* **18**, 8504–8513 (2022).
47. Harper, E. I. et al. Advanced glycation end products as a potential target for restructuring the ovarian cancer microenvironment: a pilot study. *Int. J. Mol. Sci.* **24**, 9804 (2023).
48. Charras, G. & Sahai, E. Physical influences of the extracellular environment on cell migration. *Nat. Rev. Mol. Cell Biol.* **15**, 813–824 (2014).
49. Nasser, M. W. et al. RAGE mediates S100A7-induced breast cancer growth and metastasis by modulating the tumor microenvironment. *Cancer Res* **75**, 974–985 (2015).
50. Tatsukawa, H., Furutani, Y., Hitomi, K. & Kojima, S. Transglutaminase 2 has opposing roles in the regulation of cellular functions as well as cell growth and death. *Cell Death Dis.* **7**, e2244–e2244 (2016).
51. Sima, L. E., Matei, D. & Condello, S. The outside-in journey of tissue transglutaminase in cancer. *Cells* **11**, 1779 (2022).
52. Aeschlimann, D. & Paulsson, M. Cross-linking of laminin-nidogen complexes by tissue transglutaminase. A novel mechanism for basement membrane stabilization. *J. Biol. Chem.* **266**, 15308–15317 (1991).
53. Xu, D. et al. TG2 as a novel breast cancer prognostic marker promotes cell proliferation and glycolysis by activating the MEK/ERK/LDH pathway. *BMC Cancer* **22**, 1267 (2022).
54. Iismaa, S. E., Mearns, B. M., Lorand, L. & Graham, R. M. Transglutaminases and disease: lessons from genetically engineered mouse models and inherited disorders. *Physiol. Rev.* **89**, 991–1023 (2009).
55. Schwager, S. C. et al. Weakly migratory metastatic breast cancer cells activate fibroblasts via microvesicle-Tg2 to facilitate dissemination and metastasis. *eLife* **11**, e74433 (2022).
56. Shinde, A. et al. Transglutaminase-2 facilitates extracellular vesicle-mediated establishment of the metastatic niche. *Oncogenesis* **9**, 1–12 (2020).
57. Antonyak, M. A. et al. Cancer cell-derived microvesicles induce transformation by transferring tissue transglutaminase and fibronectin to recipient cells. *Proc. Natl. Acad. Sci. USA* **108**, 4852–4857 (2011).

58. Park, S.-Y. & Nam, J.-S. The force awakens: metastatic dormant cancer cells. *Exp. Mol. Med.* **52**, 569–581 (2020).
59. Selcuk, K. et al. Transglutaminase 2 has higher affinity for relaxed than for stretched fibronectin fibers. *Matrix Biol.* **125**, 113–132 (2024).
60. Anlaş, A. A. & Nelson, C. M. Soft microenvironments induce chemoresistance by increasing autophagy downstream of integrin-linked kinase. *Cancer Res* **80**, 4103–4113 (2020).
61. Enríquez, Á. et al. High-Throughput Magnetic Actuation Platform for Evaluating the Effect of Mechanical Force on 3D tumor microenvironment. *Adv. Funct. Mater.* **31**, 2005021 (2021).
62. Wullkopf, L. et al. Cancer cells' ability to mechanically adjust to extracellular matrix stiffness correlates with their invasive potential. *Mol. Biol. Cell* **29**, 2378–2385 (2018).
63. Indra, I. & Beningo, K. A. An in vitro correlation of metastatic capacity, substrate rigidity, and ECM composition. *J. Cell. Biochem.* **112**, 3151–3158 (2011).
64. Guo, Y. et al. Different breast cancer subtypes show different metastatic patterns: a study from a large public database. *Asian Pac. J. Cancer Prev. APJCP* **21**, 3587–3593 (2020).
65. Fan, J.-H. et al. Molecular subtypes predict the preferential site of distant metastasis in advanced breast cancer: a nationwide retrospective study. *Front. Oncol*. **13** (2023).
66. Xiao, W. et al. Breast cancer subtypes and the risk of distant metastasis at initial diagnosis: a population-based study. *Cancer Manag. Res.* **10**, 5329–5338 (2018).
67. Savci-Heijink, C. D. et al. Retrospective analysis of metastatic behaviour of breast cancer subtypes. *Breast Cancer Res. Treat.* **150**, 547–557 (2015).
68. Smid, M. et al. Subtypes of breast cancer show preferential site of relapse. *Cancer Res.* **68**, 3108–3114 (2008).
69. Rostami, R., Mittal, S., Rostami, P., Tavassoli, F. & Jabbari, B. Brain metastasis in breast cancer: a comprehensive literature review. *J. Neurooncol.* **127**, 407–414 (2016).
70. Bhat, V. et al. Lung-derived soluble factors support stemness/plasticity and metastatic behaviour of breast cancer cells via the FGF2-DACH1 axis. *Clin. Exp. Metastasis* https://doi.org/10.1007/s10585-024-10284-4 (2024).
71. Ignatov, A., Eggemann, H., Burger, E. & Ignatov, T. Patterns of breast cancer relapse in accordance to biological subtype. *J. Cancer Res. Clin. Oncol.* **144**, 1347–1355 (2018).
72. Wang, H. et al. The osteogenic niche promotes early-stage bone colonization of disseminated breast cancer cells. *Cancer Cell* **27**, 193–210 (2015).
73. Gao, Y. et al. Metastasis organotropism: redefining the congenial soil. *Dev. Cell* **49**, 375–391 (2019).
74. Gao, Y., Rosen, J. M. & Zhang, X. H.-F. The tumor-immune ecosystem in shaping metastasis. *Am. J. Physiol. Cell Physiol.* **324**, C707–C717 (2023).
75. Bennett, C. et al. Breast cancer genomics: primary and most common metastases. *Cancers* **14**, 3046 (2022).
76. Fletcher, D. A. & Mullins, R. D. Cell mechanics and the cytoskeleton. *Nature* **463**, 485–492 (2010).
77. Fischer, T., Hayn, A. & Mierke, C. T. Effect of nuclear stiffness on cell mechanics and migration of human breast cancer cells. *Front. Cell Dev. Biol.* **8**, 393 (2020).
78. Tang, K., Xin, Y., Li, K., Chen, X. & Tan, Y. Cell cytoskeleton and stiffness are mechanical indicators of organotropism in breast cancer. *Biology* **10**, 259 (2021).
79. Guck, J. et al. Optical deformability as an inherent cell marker for testing malignant transformation and metastatic competence. *Biophys. J.* **88**, 3689–3698 (2005).
80. Suresh, S. Biomechanics and biophysics of cancer cells. *Acta Biomater.* **3**, 413–438 (2007).
81. Plodinec, M. et al. The nanomechanical signature of breast cancer. *Nat. Nanotechnol.* **7**, 757–765 (2012).
82. Swaminathan, V. et al. Mechanical stiffness grades metastatic potential in patient tumor cells and in cancer cell lines. *Cancer Res.* **71**, 5075–5080 (2011).
83. Lv, J. et al. Cell softness regulates tumorigenicity and stemness of cancer cells. *EMBO J.* **40**, e106123 (2021).
84. Castro, D. J., Maurer, J., Hebbard, L. & Oshima, R. G. ROCK1 inhibition promotes the self-renewal of a novel mouse mammary cancer stem cell. *Stem Cells Dayt. Ohio* **31**, 12–22 (2013).
85. Luo, Q., Kuang, D., Zhang, B. & Song, G. Cell stiffness determined by atomic force microscopy and its correlation with cell motility. *Biochim. Biophys. Acta* **1860**, 1953–1960 (2016).
86. Chen, X. et al. The mechanics of tumor cells dictate malignancy via cytoskeleton-mediated APC/Wnt/β-catenin signaling. *Research* **6**, 0224 (2023).
87. Jin, J., Tang, K., Xin, Y., Zhang, T. & Tan, Y. Hemodynamic shear flow regulates biophysical characteristics and functions of circulating breast tumor cells reminiscent of brain metastasis. *Soft Matter* **14**, 9528–9533 (2018).
88. Xin, Y. et al. Mechanics and actomyosin-dependent survival/chemoresistance of suspended tumor cells in shear flow. *Biophys. J.* **116**, 1803–1814 (2019).
89. DeCastro, A. J. L. et al. Morphological phenotyping of organotropic brain- and bone-seeking triple negative metastatic breast tumor cells. *Front. Cell Dev. Biol.* **10**, 790410 (2022).
90. Gao, W. et al. Isolation and phenotypic characterization of colorectal cancer stem cells with organ-specific metastatic potential. *Gastroenterology* **145**, 636–646.e5 (2013).
91. Savci-Heijink, C. D., Halfwerk, H., Koster, J. & van de Vijver, M. J. A novel gene expression signature for bone metastasis in breast carcinomas. *Breast Cancer Res. Treat.* **156**, 249–259 (2016).
92. Savci-Heijink, C. D., Halfwerk, H., Koster, J., Horlings, H. M. & van de Vijver, M. J. A specific gene expression signature for visceral organ metastasis in breast cancer. *BMC Cancer* **19**, 333 (2019).
93. Zhang, B. et al. Adhesion to the brain endothelium selects breast cancer cells with brain metastasis potential. *Int. J. Mol. Sci.* **24**, 7087 (2023).
94. Osmani, N. et al. Metastatic tumor cells exploit their adhesion repertoire to counteract shear forces during intravascular arrest. *Cell Rep.* **28**, 2491–2500.e5 (2019).
95. Anvari, S., Osei, E. & Maftoon, N. Interactions of platelets with circulating tumor cells contribute to cancer metastasis. *Sci. Rep.* **11**, 15477 (2021).
96. Kang, S.-A. et al. Blocking the adhesion cascade at the premetastatic niche for prevention of breast cancer metastasis. *Mol. Ther.* **23**, 1044–1054 (2015).
97. Rahn, J. J. et al. MUC1 mediates transendothelial migration in vitro by ligating endothelial cell ICAM-1. *Clin. Exp. Metastasis* **22**, 475–483 (2005).
98. Ji, S., Wu, W. & Jiang, Q. Crosstalk between endothelial cells and tumor cells: a new era in prostate cancer progression. *Int. J. Mol. Sci.* **24**, 16893 (2023).
99. Taftaf, R. et al. ICAM1 initiates CTC cluster formation and trans-endothelial migration in lung metastasis of breast cancer. *Nat. Commun.* **12**, 4867 (2021).
100. Chen, Q., Zhang, X. H.-F. & Massagué, J. Macrophage binding to receptor VCAM-1 transmits survival signals in breast cancer cells that invade the lungs. *Cancer Cell* **20**, 538–549 (2011).
101. Zhan, Q. et al. New insights into the correlations between circulating tumor cells and target organ metastasis. *Signal Transduct. Target. Ther.* **8**, 1–23 (2023).
102. Feng, W., Chen, L., Nguyen, P. K., Wu, S. M. & Li, G. Single cell analysis of endothelial cells identified organ-specific molecular

signatures and heart-specific cell populations and molecular features. *Front. Cardiovasc. Med*. **6** (2019).
103. Pereira, E. R. et al. Lymph node metastases can invade local blood vessels, exit the node and colonize distant organs in mice. *Science* **359**, 1403–1407 (2018).
104. Naxerova, K. et al. Origins of lymphatic and distant metastases in human colorectal cancer. *Science* **357**, 55–60 (2017).
105. Rezzola, S., Sigmund, E. C., Halin, C. & Ronca, R. The lymphatic vasculature: an active and dynamic player in cancer progression. *Med. Res. Rev.* **42**, 576–614 (2022).
106. Lee, H. J. et al. Fluid shear stress activates YAP1 to promote cancer cell motility. *Nat. Commun.* **8**, 14122 (2017).
107. Lee, H. J., Ewere, A., Diaz, M. F. & Wenzel, P. L. TAZ responds to fluid shear stress to regulate the cell cycle. *Cell Cycle* **17**, 147–153 (2018).
108. Kawai, Y., Kaidoh, M., Yokoyama, Y. & Ohhashi, T. Pivotal roles of shear stress in the microenvironmental changes that occur within sentinel lymph nodes. *Cancer Sci.* **103**, 1245–1252 (2012).
109. Shinde, A. et al. Autocrine fibronectin inhibits breast cancer metastasis. *Mol. Cancer Res.* **16**, 1579–1589 (2018).
110. Qian, J. J. & Akçay, E. Competition and niche construction in a model of cancer metastasis. *PLoS ONE* **13**, e0198163 (2018).
111. Morris, V. L. et al. Mammary carcinoma cell lines of high and low metastatic potential differ not in extravasation but in subsequent migration and growth. *Clin. Exp. Metastasis* **12**, 357–367 (1994).
112. Martin, M. D. et al. Rapid extravasation and establishment of breast cancer micrometastases in the liver microenvironment. *Mol. Cancer Res.* **8**, 1319–1327 (2010).
113. Chen, W., Hoffmann, A. D., Liu, H. & Liu, X. Organotropism: new insights into molecular mechanisms of breast cancer metastasis. *Npj Precis. Oncol.* **2**, 1–12 (2018).
114. Cameron, M. D. et al. Temporal progression of metastasis in lung: cell survival, dormancy, and location dependence of metastatic inefficiency1. *Cancer Res.* **60**, 2541–2546 (2000).
115. Chu, H.-Y. et al. Physical cues in the microenvironment regulate stemness-dependent homing of breast cancer cells. *Cancers* **12**, 2176 (2020).
116. Watson, A. W. et al. Breast tumor stiffness instructs bone metastasis via maintenance of mechanical conditioning. *Cell Rep*. **35** (2021).
117. Rozova, V. S. et al. Machine learning reveals mesenchymal breast carcinoma cell adaptation in response to matrix stiffness. *PLoS Comput. Biol.* **17**, e1009193 (2021).
118. Akhmetkaliyev, A., Alibrahim, N., Shafiee, D. & Tulchinsky, E. EMT/MET plasticity in cancer and Go-or-Grow decisions in quiescence: the two sides of the same coin? *Mol. Cancer* **22**, 90 (2023).
119. Tachtsidis, A. et al. Human-specific RNA analysis shows uncoupled epithelial-mesenchymal plasticity in circulating and disseminated tumour cells from human breast cancer xenografts. *Clin. Exp. Metastasis* **36**, 393–409 (2019).
120. Zanotelli, M. R. et al. Highly motile cells are metabolically responsive to collagen density. *Proc. Natl. Acad. Sci. USA* **119**, e2114672119 (2022).

Acknowledgements

This work was supported by the National Cancer Institute CA264734 to S.L. Figures 1 and 2 were adapted under CC BY 4.0[15,26,78] (https://creativecommons.org/licenses/by/4.0/) and Fig. 3 was created with BioRender.com.

Author contributions

S.L. and C.A.R. developed the basis of the article, S.L. wrote the main text and prepared the figures, C.A.R. edited the main text.

Competing interests

The authors declare no competing interests.

Additional information

Correspondence and requests for materials should be addressed to Cynthia A. Reinhart-King.